

Disruption Thermal Quench Mitigation by Noble Gas Jet Injection Ex-S

E.M. Hollmann¹, D.S. Gray¹, D.G. Whyte², T.C. Jernigan³, M. Groth⁴, D.A. Humphreys⁵, P.B. Parks⁵, T.E. Evans⁵, C.J. Lasnier⁴, D.L. Rudakov¹, R.A. Moyer¹, N.H. Brooks⁵, and A. McLean⁶

¹University of California-San Diego, La Jolla, California 92093, USA
email: ehollmann@ucsd.edu

²University of Wisconsin-Madison, Madison, Wisconsin 53706, USA

³Oak Ridge National Laboratory, Oak Ridge, Tennessee 37831, USA

⁴Lawrence Livermore National Laboratory, Livermore, California, 94550, USA

⁵General Atomics, San Diego, California 92186, USA

⁶University of Toronto, Toronto, Ontario M5S1A1, Canada

In next-generation tokamaks like ITER, it is expected that a single disruption will release thermal energies of order 0.5 GJ, with a fraction (perhaps 1/4) of this energy coming out during a slow (~10-20 ms) precursor phase and the balance coming out in a more rapid (~1 ms) thermal quench spike. These heat loads have the potential to severely damage the vessel walls, especially if the deposition is strongly localized. Developing a disruption mitigation technique which ensures uniform wall heating and, if possible, lengthens the timescale of the thermal quench spike is a challenging and critical issue for future tokamaks.

High-pressure noble gas injection is a promising candidate for disruption mitigation, since noble gas jet injection experiments have demonstrated rapid termination of discharges while avoiding halo currents and runaway electron generation during the disruption current quench phase [1]. The gas jet impurities reach the plasma core on a timescale of several ms, so this technique is expected to be fast enough for thermal quench mitigation in large tokamaks.

Here it is shown that noble gas injection in DIII-D provides good thermal quench mitigation, i.e. the initial thermal energy is lost by radiation (which causes uniform wall heating), rather than by conduction (which gives very localized wall heating). Figure 1(a) shows the thermal quench radiated power P_{rad} obtained from fast bolometry [2] as a function of initial thermal energy W_0 . It can be seen that the mitigated disruptions (open circles) typically have a radiated power fraction of nearly 100%, while normal disruptions (solid circles) average around 40% radiated power fraction (with radiation coming dominantly from carbon sputtered from the vessel walls). The remaining energy must be conducted to the vessel walls and divertor, resulting in very non-uniform heat loads. Figure 1(b) shows the main chamber radiated power fraction, demonstrating that very little heat flow into the divertor occurs during the mitigated disruptions.

Understanding the mechanisms by which the gas jet impurities move into the plasma core is crucial for extrapolating this technique to larger machines. In DIII-D, this transport appears

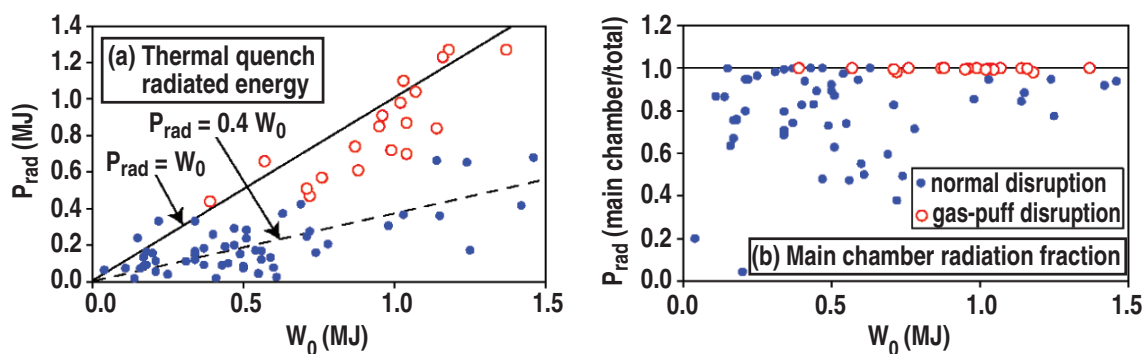


Fig. 1. (a) Total (main chamber plus divertor) thermal quench radiated power and (b) Main chamber thermal quench radiated power normalized by total (main chamber plus divertor) thermal quench radiated power, both as a function of initial stored thermal energy.

to take place in three stages: direct neutral propagation across the plasma edge, followed by slow impurity ion transport across the pedestal, followed by a fast mixing of impurity ions into the core plasma.

Initially, the jet neutrals travel freely across the plasma edge. In the SOL, the ablation cloud pressure due to the plasma-jet interaction [3] is somewhat less than the jet ram pressure ($\sim 0.2\text{-}0.5$ atm) so the jet neutrals can transit this region ballistically.

Upon reaching the pedestal, the neutrals are stopped and begin spreading poloidally and toroidally; this is observed by fast-gated CID camera imaging of the jet neutral line emission. The pedestal temperature profile and plasma current channel shrink as heat is transported outward from the pedestal into the cold impurity cloud at the edge of the plasma; this is seen from Thomson scattering bursts and from a slight increase in the plasma self-inductance. Impurity neutrals remain localized to the plasma edge in the vicinity of the jet port. However, low charge-state impurity ions beginning spreading toroidally along the magnetic field lines; this is observed with CID camera imaging of ion line emission, with fast visible spectrometers, and with fast bolometry. Fast ECE measurements show that the core electron temperature remains relatively unperturbed at this point.

After about 4-5 ms, the collapsing cold front reaches $q \approx 2$, initiating a flurry of MHD activity. The dominant initial mode usually appears to be a (2/1) tearing mode; however, the MHD activity is quickly driven into broadband turbulence. The hot core plasma and the cold impurity ions from the edge region are mixed together and the plasma thermal energy is radiated away in a sharp thermal quench radiation spike. This mixing of impurity ions into the core plasma can be seen with fast bolometry of the radiated power profile. VUV spectroscopy shows the appearance of high impurity charge states (e.g. Ne-VIII) at this point, consistent with impurities mixing into the hot core plasma. Anomalous ion transport from motion along ergodic field lines is estimated using the standard technique of integrating wall B_r fluctuations and is found to be too small to be significant here. However, direct cross-field transport of impurities through entrainment in the MHD turbulence is found to be large enough to explain the observed transport, as shown in Fig. 2.

The relevance of these measurements to ITER will be discussed, as well as additional work presently in progress, which includes noble gas injection using a nozzle with higher initial ram pressure and investigations into the possibility of using liquid jets.

Work supported by U. S. Department of Energy under Grant Nos. DE-FG02-04ER-54758, DE-FG02-89ER53297, Contract Nos. DE-FC05-00OR22725, W-7405-ENG-48, and Cooperative Agreement DE-FC02-04ER54698.

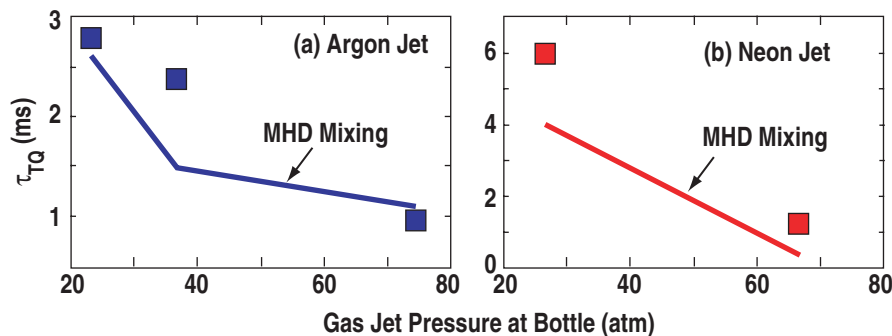


Fig. 2. Measured core thermal collapse time τ_{TQ} compared with MHD mixing time from SXR tomography as a function of jet pressure at gas bottle for (a) argon injection and (b) neon injection.

- [1] D.G. Whyte, T.C. Jernigan, D.A. Humphreys, *et al.*, J. Nucl. Mater. **313**, 1239 (2003).
- [2] E.M. Hollmann, D.S. Gray, D.G. Whyte, *et al.*, Phys. Plasmas **10**, 2863 (2003).
- [3] P.B. Parks and R.J. Turnbull, Phys. Fluids **21**, 1735 (1978).